



Effects of insulin and metformin on fetal kidney development of streptozotocin-induced gestational diabetic albino rats

Ban M. Kassab, Hoda H. Hussein, Omayma M. Mahmoud, Gamal Abdel-Alrahman

Department of Anatomy, Faculty of Medicine, Suez Canal University, Ismailia, Egypt

Abstract: Gestational diabetes mellitus is one of common medical complications of pregnancy. Hyperglycemia in utero impairs renal development and produces renal anomalies. Metformin has antioxidant properties and better glycemic control. Aim: assessment insulin and metformin effects on renal development of streptozotocin-induced gestational diabetic albino rats. Sixty virgin female albino rats were used. Once pregnancy confirmed, animals were randomly assigned into control, metformin, diabetic, diabetic plus insulin, diabetic plus metformin and diabetic plus insulin and metformin treated groups. Rats were sacrificed on the 20th day of gestation; fetuses were extracted and weighted. Fetal kidneys were extracted prepared for light, morphometric and electron microscopic examination. Diabetic followed by diabetic plus metformin treated groups revealed retardation of glomerular development in the cortical and Juxtaglomerular zones with a significant increase in the early immature glomerular stages and immature to mature glomerular ratio compared to other groups. Diabetic group also showed morphometric changes, shrunken and empty glomeruli, vacuolar degeneration and hemorrhage. Diabetic plus metformin group showed minimal improvement while diabetic plus insulin and diabetic plus insulin and metformin groups showed developmental, histopathological and morphometric improvement with best results in the combination group. Gestational diabetes mellitus (GDM) possess deleterious effects on fetal kidney development. Insulin improves the glycemic state and decreases GDM effects on fetal kidneys. Metformin produces mild protection while the combination of insulin and metformin produces the best glycemic control and protect fetal kidneys.

Key words: Gestational diabetes mellitus, Insulin, Metformin, Kidney development, Albino rat

Received October 23, 2018; 1st Revised November 21, 2018; 2nd Revised December 12, 2018; Accepted December 14, 2018

Introduction

Diabetes mellitus (DM) is a group of metabolic disorders which characterized by high glucose levels due to insufficiency in production or action of insulin [1]. Animal models of

DM are currently used in researches such as feeding of high energy diet in sand rats (*Psammomys obesus*) as a model for type 2 DM and treatment with streptozotocin (STZ) which represents the well-established model of type 1 DM [2, 3].

DM is associated with metabolic and haemodynamic stresses which induce alterations to DNA, proteins, lipids, cellular damage and stimulate inflammatory and fibrotic responses leading to various types of renal injury [4]. Gestational diabetes mellitus (GDM) is one of the most common medical complications of pregnancy. It is defined as “any grade of glucose intolerance with beginning or first recognition during pregnancy” [5]. Babies born to women with elevated blood glucose levels are at greater risk of foetal abnormalities [6].

Corresponding author:

Omayma M. Mahmoud
Department of Anatomy, Faculty of Medicine, Suez Canal University,
Ring road, kilo 4.5, Ismailia 41111, Egypt
Tel: +20-01272759000, Fax: +20-20643208543, E-mail: omima34@hotmail.com

Copyright © 2019. Anatomy & Cell Biology

This is an Open Access article distributed under the terms of the Creative Commons Attribution Non-Commercial License (<http://creativecommons.org/licenses/by-nc/4.0/>) which permits unrestricted non-commercial use, distribution, and reproduction in any medium, provided the original work is properly cited.

Organogenesis may be significantly affected when diabetes starts at an early phase of pregnancy [7]. Human renal development occurs at fifth week of gestation while in rats it starts at the 12th day of gestation [8]. Hyperglycemia *in utero* impairs renal development and cause renal anomalies. Since GDM is characterized by insulin resistance (IR) and relatively decreased insulin secretion, a treatment with non-insulin antihyperglycemic agents could be of a potential interest. The main concern of using non-insulin antihyperglycemic agents in pregnancy is congenital anomalies and fetal hypoglycemia [9].

Metformin (dimethyl-biguanide) is an insulin-sensitizing agent that lowers fasting plasma glucose concentration by increasing the peripheral uptake of glucose and decreasing hepatic glucose output [10]. Metformin eliminates the symptoms of DM and located at category B drug indicating that it has no evidence of teratogenicity [11]. Treatment of GDM with metformin decreased the rates of spontaneous abortion, induced normal growth and development of the offspring and favorable pregnancy outcomes [12]. Some authors reported that half of patients with GDM who were initially treated with metformin needed insulin in order to achieve acceptable glucose control [13]. Metformin has antioxidant properties that protect the body against insulin mediated oxidative damage and stress [14]. Therefore, this study was conducted to assess the effect of insulin and metformin on the development of 20 days fetal kidneys of STZ-induced gestational diabetic albino rats.

Materials and Methods

Chemicals and drugs

STZ obtained from Sigma-Aldrich (St. Louis, MO, USA). Insulin (Lantus 100 U/ml) obtained from SANOFI Aventis (Cairo, Egypt) and metformin was obtained from Holdi-pharma (Cairo, Egypt).

Animals

Sixty virgin females and 10 males Sprague-Dawley albino rats (weighting 150–200 g and aged 10–12 weeks) were obtained from animal house of Faculty of Veterinary Medicine, Suez Canal University, Ismailia, Egypt and used throughout the study. All animals were left in the animal house of the Department of Human Anatomy and Embryology, Faculty of Medicine, Suez Canal University for 2 weeks for acclimatization. They were housed in spacious wire mesh cages in a good

ventilated room 12-hour light/dark cycle and received water and food ad libitum. Mating was carried out by introducing one male into a cage with two female rats and left them overnight. vaginal smears were taken in the following morning and pregnancy verified by the presence of spermatozoa which indicated the first day of gestation (GD1) [15].

Experimental design

Once pregnancy was confirmed, animals were randomly assigned to six groups: (1) control group (C), (2) metformin-treated group (M), (3) diabetic group (D), (4) diabetic plus insulin-treated group (D+I), (5) diabetic plus metformin-treated group (D+M), and (6) diabetic plus insulin and metformin-treated group (D+I+M). Each group consisted of 10 pregnant female rats.

Induction of DM

Single intraperitoneal injection of STZ (35 mg/kg body weight) on the seventh day of gestation in groups 3, 4, 5, and 6. Blood glucose level was measured daily through tail vein 3 days after STZ injection. Rats with blood glucose levels exceeding 200 mg/dl were considered as diabetic [16].

Animal treatment

- Control group (C): pregnant rats with blood glucose level less than 200 mg/dl was divided into two subgroups: positive control (C+ve), animals received single dose of citrate buffer (pH 4.5) 0.2 ml/100 g body weight intraperitoneally; negative control (C-ve), animals didn't receive any treatment.

- Metformin-treated group (M): pregnant non-diabetic rats received intra-gastric metformin (250 mg/kg body weight) daily [17].

- Diabetic group (D): pregnant diabetic rats with glucose level more than 200 mg/dl.

Diabetic plus insulin-treated group (D+I): pregnant diabetic rats received insulin 14 IU/kg daily [18].

- Diabetic plus metformin-treated group (D+M): pregnant diabetic rats received intra-gastric metformin (250 mg/kg body weight) daily.

- Diabetic plus insulin and metformin-treated group (D+I+M): pregnant diabetic rats received insulin (7 IU/kg body weight daily) and metformin (125 mg/kg body weight daily).

Insulin and metformin were given to pregnant rats from the 11th day to 20th day of gestation.

Experimental evaluation

Random blood sugar level was measured and recorded for all pregnant rats from the beginning to the end of the experiment. The pregnant rats were euthanized and sacrificed on the 20th day of gestation by cervical dislocation. Fetuses were obtained by caesarian section. The numbers of live, dead fetuses and metrial glands were recorded. Fetuses were weighted, euthanized and sacrificed by decapitation and kidneys were collected. Placental weight was also measured. Fetal kidneys width and length were measured with micrometer in the eyepiece of the dissecting microscope [19].

Histological assessment of fetal kidneys

Light microscopic assessment

Right kidneys were collected and prepared for light microscopic examination. They were fixed in 4% paraformaldehyde and then embedded in paraffin blocks. Transverse sections 4 μ m thickness were cut and stained using hematoxylin and eosin (H&E) and periodic acid–Schiff (PAS) stains [20].

Morphometric assessment

In H&E stained sections of the fetal kidneys the following parameters were measured:

- Cortical thickness was measured at a magnification of $\times 100$.
- Diameter of glomeruli, renal corpuscle, Proximal and distal tubule were measured at the magnification of $\times 400$.
- Glomerular maturation: number of mature and immature glomeruli was counted in at magnification of $\times 400$.

Morphometric parameters were measured by micrometre lens in the eyepiece of Olympus light microscope (Tokyo, Japan). Five fields from five serial sections in each kidney were used [21].

Electron microscopic assessment

Left kidneys were divided into small pieces, fixed in buffered glutaraldehyde 2.5% for two hours and fixed in 1% osmic tetroxide. After dehydration in ascending grades of cold ethanol and propylene oxide, the specimens were embedded in Spurr's resin. Semithin sections stained with toluidine blue were examined by light microscope. Ultrathin sections were cut using MT 600-XL RMC ultra-tome (Tokyo, Japan) and stained with uranyl acetate and lead citrate and examined with JEOL-1010 (Tokyo, Japan) transmission electron micro-

scope, at the regional centre of mycology and biotechnology transmitting electron unit, Alazhar University, Cairo, Egypt.

Statistical analysis

Results were analysed using the SPSS ver. 21 (IBM Corp., Armonk, NY, USA). Differences between groups were tested using one-way analysis of variance (ANOVA) and chi square tests. Probability values (*P*) less than 0.05 were considered statistically significant.

Ethical consideration

All authors declare that all experiments had performed under the ethical standards and approved by an animal use and care committee of Suez Canal University and we have respected the ethical principles underpinning the research.

Results

Random blood sugar level

Random blood sugar (RBS) levels were within normal range in all rats of all studied groups at the beginning of pregnancy (GD1). Control (C-ve and C+ve) and M-treated groups showed normal levels of RBS throughout gestation. Diabetic groups (D, D+I, D+M, and D+I+M) showed an increase in RBS level after the induction of diabetes until GD10, whereas D group only continued the increase in RBS level until GD20.

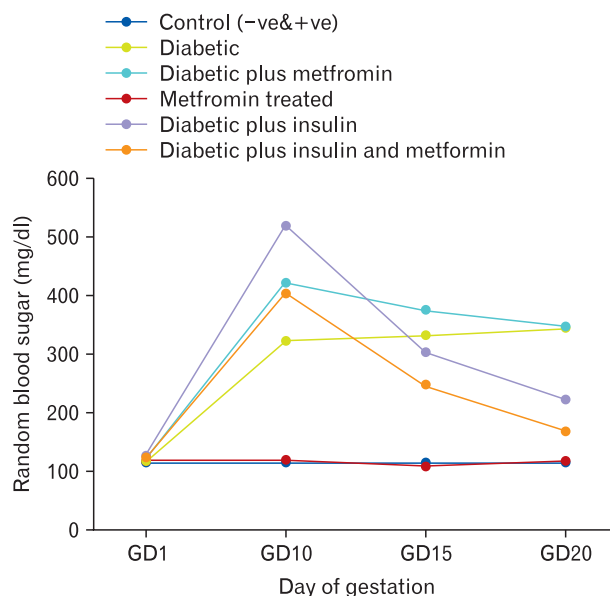


Fig. 1. Values of maternal random blood sugar throughout gestation in the studied groups. +ve, positive control; -ve, negative control.

Others diabetic treated rats (D+I, D+M, and D+I+M) showed a decrease in the hyperglycaemia after the initiation of treatment with insulin and metformin (from GD10 to GD20) with more decrease in D+I and D+I+M treated group than the levels of D+M treated group. The best and closest value of RBS to the control in the day of scarification (GD20) was in the D+I+M treated group (Fig. 1).

Embryolethality

The post-implantation resorptions were significantly increased in D, D+I, D+M, and D+I+M treated groups when compared to both control and metformin groups (Table 1). Moreover, D+I, D+M, and D+I+M treated groups revealed a significant decrease in post-implantation resorptions compared to diabetic group with more decrease in D+I+M treated group. Furthermore, D+I and D+I+M treated groups showed a significant decrease in resorption compared to D+M treated group (Table 1).

Table 1. Frequency of embryolethality in studied groups

Group	Live fetuses (%)	Dead fetuses (%)	Post-implantation resorptions (%)
Control			
C-ve	100	0	0
C+ve	100	0	0
Metformin	100	0	0
Diabetic	30.8	10.7	58.5 ^{a),b)}
Diabetic+insulin	66.7	0	33.3 ^{a),b),c),e)}
Diabetic+metformin	40.4	0	59.6 ^{a),b),c),d)}
Diabetic+insulin+metformin	90.5	0	9.5 ^{a),b),c),d),e)}

Chi-square test. C+ve, positive control; C-ve, negative control. ^{a)}P<0.05 compared to control groups. ^{b)}P<0.05 compared to Metformin treated group. ^{c)}P<0.05 compared to diabetic group. ^{d)}P<0.05 compared to diabetic plus insulin treated group. ^{e)}P<0.05 compared to diabetic plus metformin treated group.

Table 2. Changes in fetal body and placental weights in all studied groups

Group	Fetal weight (g)	Placental weight (g)
Control		
C-ve	3.19±0.12	0.48±0.08
C+ve	3.18±0.11	0.49±0.03
Metformin treated	3.24±0.12	0.51±0.08
Diabetic	4.95±0.14 ^{a),b),d),e),f)}	0.78±0.08 ^{a),b),d),e),f)}
Diabetic+insulin	4.39±0.16 ^{a),b),c),e),f)}	0.67±0.09 ^{a),b),c),e)}
Diabetic+metformin	4.04±0.14 ^{a),b),c),d),f)}	0.6±0.09 ^{a),c)}
Diabetic+insulin+metformin	3.49±0.16 ^{a),b),c),d),e)}	0.57±0.08 ^{c),d)}

Values are presented as mean±SD. ANOVA *post hoc* test. C+ve, positive control; C-ve, negative control. ^{a)}P<0.05 compared to control groups. ^{b)}P<0.05 compared to metformin treated group. ^{c)}P<0.05 compared to diabetic group. ^{d)}P<0.05 compared to diabetic plus insulin treated group. ^{e)}P<0.05 compared to diabetic plus metformin treated group. ^{f)}P<0.05 compared to diabetic plus insulin and metformin treated group.

Foetal body and placental weights

All foetuses of D, D+I, D+M, and D+I+M treated groups showed a significant increase in foetal body weight and placental weight compared to control and metformin treated groups. Moreover, D+I, D+M, and D+I+M treated groups showed a significant decrease in fetal and placental weights compared to D group. Furthermore, D+I+M treated group showed a significant decrease in fetal and placental weights compared to D+M and D+I treated groups (Table 2).

Gross morphological results of fetal kidneys

Both length and width of fetal kidneys were significantly increased in D, D+I, and D+M treated groups compared to control and M treated groups. Moreover, D+I and D+I+M treated groups showed a significant decrease in fetal kidney length and width compared to D group. Furthermore, D+I+M treated group revealed a significant decrease in fetal kidney growth parameters compared to D+I and D+M treated groups and close to the values of control and M treated group (Table 3).

Morphometric results of foetal kidneys

Diabetic, D+I and D+M treated groups showed significant increase in the cortical thickness, corpuscular diameter, and tubular diameter (proximal convoluted tubule and distal convoluted tubule) of foetal kidneys and significant decrease in the glomerular diameter compared to control and M treated groups. Moreover, D+I, D+M, and D+I+M treated groups revealed significant decrease in cortical thickness, corpuscular diameter and tubular diameter of foetal kidneys and significant increase in glomerular diameter compared to diabetic

Table 3. Length and width of fetal kidneys in all studied groups

Group	Fetal kidney length (mm)	Fetal kidney width (mm)
Control		
C-ve	3.25±0.01	2.2±0.08
C+ve	3.25±0.04	2.19±0.01
Metformin treated	3.26±0.01	2.08±0.01
Diabetic	3.49±0.02 ^{a),b),d),e),f)}	2.36±0.05 ^{a),b),d),e),f)}
Diabetic+insulin	3.31±0.04 ^{a),b),c),f)}	2.17±0.07 ^{b),c),e),f)}
Diabetic+metformin	3.42±0.03 ^{a),b),d),f)}	2.29±0.02 ^{a),b),c),d),f)}
Diabetic+insulin+metformin	3.28±0.02 ^{c),d),e)}	2.09±0.0 ^{a),b),c),e)}

Values are presented as mean±SD. ANOVA *post hoc* test. C+ve, positive control; C-ve, negative control. ^{a)}P<0.05 compared to control groups. ^{b)}P<0.05 compared to metformin treated group. ^{c)}P<0.05 compared to diabetic group. ^{d)}P<0.05 compared to diabetic plus insulin treated group. ^{e)}P<0.05 compared to diabetic plus metformin treated group. ^{f)}P<0.05 compared to diabetic plus insulin and metformin treated group.

Table 4. Morphometric parameters of fetal kidneys

Group	Cortical thickness (μm)	Corpuscular diameter (μm)	Glomerular diameter (μm)	PCT diameter (μm)	DCT diameter (μm)
Control					
C-ve	675.34 \pm 53.91	55.75 \pm 2.13	37.43 \pm 2.1	17.43 \pm 1.61	17.07 \pm 1.36
C+ve	674.51 \pm 51.31	54.28 \pm 2.07	37.03 \pm 1.9	17 \pm 1.21	18.11 \pm 1.61
Metformin	676.85 \pm 45.05	56.34 \pm 1.72	37.09 \pm 2.27	18 \pm 1.23	18.94 \pm 0.97
Diabetic	1412.97 \pm 121.5 ^{a),(b),(d),(e),(f)}	81.19 \pm 3.22 ^{a),(b),(d),(e),(f)}	20.61 \pm 2.23 ^{a),(b),(d),(e)}	36.16 \pm 6.76 ^{a),(b),(e)}	36.49 \pm 4.31 ^{a),(b),(d),(e),(f)}
Diabetic+insulin	947.57 \pm 46.76 ^{a),(b),(c),(e),(f)}	61.09 \pm 7.4 ^{(c),(f)}	31 \pm 1.24 ^{a),(b),(c),(e),(f)}	28.2 \pm 6.4 ^{a),(b),(e)}	26.53 \pm 6.18 ^{a),(b),(c),(e)}
Diabetic+metformin	1269.89 \pm 66.38 ^{a),(b),(c),(d),(f)}	71.19 \pm 1.87 ^{a),(b),(c),(d),(f)}	21.11 \pm 2.37 ^{a),(b),(c),(d),(f)}	31.24 \pm 2.31 ^{a),(b),(f)}	30.13 \pm 1.18 ^{a),(b),(c),(f)}
Diabetic+insulin+metformin	869.45 \pm 29.99 ^{a),(b),(c),(d),(e)}	57.52 \pm 2.64 ^{(c),(e)}	36.53 \pm 1.43 ^{a),(c),(d),(e)}	20.71 \pm 2 ^{a),(b),(c),(d),(e)}	19.05 \pm 1.84 ^{(c),(d),(e)}

Values are presented as mean \pm SD. ANOVA *post hoc* test. PCT, proximal convoluted tubule; DCT, distal convoluted tubule; C+ve, positive control; C-ve, negative control. ^{a)} $P < 0.05$ compared to control groups. ^{b)} $P < 0.05$ compared to metformin treated group. ^{c)} $P < 0.05$ compared to diabetic group. ^{d)} $P < 0.05$ compared to diabetic plus insulin treated group. ^{e)} $P < 0.05$ compared to diabetic plus metformin treated group. ^{f)} $P < 0.05$ compared to diabetic plus insulin and metformin treated group.

group. Furthermore, D+I+M treated followed by D+I treated groups revealed significant improvement in these parameters compared to D+M treated group (Table 4).

Glomerular maturation

The number of total and cortical immature glomeruli was significantly increased in diabetic and D+M treated groups compared to other groups. Diabetic group followed by D+M treated group also revealed significant increase in the early stages of glomerular development (vesicle, S-shaped, and comma shaped glomeruli) and marked decrease in the number of mature glomeruli (total, cortical and juxtaglomerular) with an increase in ratio between the immature and mature glomeruli compared to other groups.

Moreover, D+I treated group showed significant decrease in the total and cortical immature glomeruli and significant increased number of immature glomeruli of the juxtaglomerular zone compared to the diabetic group. They also revealed significant decrease in the number of early glomerular stages and significant increase in the number of capillary loop glomerular stage and mature glomeruli (total, cortical, and juxtaglomerular) compared to diabetic group, with a decrease in the immature/mature glomerular ratio.

Furthermore, D+I+M treated group revealed significantly decreased number of total and cortical immature glomeruli compared to diabetic and D+M treated groups. D+I+M treated group also showed significant decrease in the immature forms and significant increase in the number mature glomeruli (total, cortical, and juxtaglomerular) compared to other diabetic groups with a decrease in the immature/mature glomerular ratio to the closest value to the control group (Table 5).

Histopathological results

Control group

H&E-stained sections of the fetal kidneys in control group (negative and positive subgroups) showed clearly defined cortex and medulla. The cortex consisted of immature and mature renal corpuscles, along with the convoluted tubules. The immature renal corpuscles showed different stages of development: Vesicle stage, early S-shape, or comma shape stage, late S-shape stage and capillary loop stage. The mature renal corpuscle is a rounded structure, composed of a tuft of glomerular capillaries, which is invaginated into the Bowman's capsule and separated from it by Bowman's space (corpuscular space). The convoluted tubules are differentiated into proximal and distal convoluted tubules. The proximal convoluted tubules composed of simple cuboidal epithelial cells with eosinophilic and granular cytoplasm. The distal convoluted tubules have wide lumina and lined with low cuboidal epithelium with pale granular cytoplasm (Fig. 2). Examination of PAS stained sections revealed positive PAS stain in the glomeruli, Bowman's capsule, basement membrane and the brush border of the proximal convoluted tubules (Fig. 3). Toluidine blue-stained sections showed mature, immature renal corpuscles with different stages of glomerular development and convoluted tubules. The mature renal corpuscle is composed of a tuft of glomerular capillaries surrounded by flat podocytes and mesangial cells and invaginated into the Bowman's capsule (Fig. 4).

The ultrastructure of fetal kidneys in control group (negative and positive subgroups) showed glomerular capillaries, lined with endothelial cells forming fenestrated endothelial layer and rested on a basement membrane. The glomerular capillaries were surrounded by flat podocytes with foot pro-

Table 5. Number of immature and mature glomeruli in the studied groups

Group	No. of immature glomeruli				No. of immature glomerular stages				No. of mature glomeruli			Immature/ mature glomerular ratio
	Total	Cortical zone	Juxtglomerular zone	Vesicle stage	S shaped stage	Comma shaped stage	Capillary loop stage	Total	Cortical zone	Juxtglomerular zone	Immature/ mature glomerular ratio	
Control												
C+ve	44.4±13	31.8 ±10	12.6±9.7	12±4.7	8.2±3	11.6±2.6	12.6±9.7	68.4±3.8	33.1±1.8	35.3±2.0	0.6	
C-ve	45.0±11	32.6±9	12.4±3.8	12±3.2	8.9±2.2	11.7±2.8	12.4±3.8	67.9±4.4	31.4±2.1	36.5±2.2	0.7	
Metformin	47.6±7.3	33.6±6.1	14±3.4	11.2±3.4	10.2±2.4	12.2±1.3	14±3.4	63.2±5.8	29±3.5	34.2±5.3	0.7	
Diabetic	86.8±19 ^(a,b)	76±18.4 ^(a,b)	10.8±4.5	26.2±10.9 ^(a,b)	21.8±6.6 ^(a,b)	28±3.4 ^(a,b)	10.8±4.5	13.6±2.7 ^(a,b)	4.2±1.9 ^(a,b)	9.4±0.8 ^(a,b)	6.4	
Diabetic+insulin	59.6±2.7 ^(c)	34.8±1.7 ^(c)	24.8±2.2 ^(a,b,c,e)	8.8±3.6 ^(c)	9.4±4.2 ^(c)	16.6±3.6 ^(a,b,c)	24.8±2.2 ^(a,b,b,c)	40.4±7.2 ^(a,b,b,c)	20±3.9 ^(a,b,c)	20.4±3.3 ^(a,b,c)	1.5	
Diabetic+metformin	72.4±10.4 ^(a,b)	59.4±8.2 ^(a,b)	13±7.3	25.4±10.1 ^(a,b,b,d)	18.6±1.9 ^(a,b,b,d)	15.4±3.2 ^(c)	13±7.3 ^(d)	24.8±2.8 ^(a,b,c,d)	7.5±1.8 ^(a,b,b,d)	17.3±1.0 ^(a,b,c)	3.0	
Diabetic+insulin+metformin	54.2±3.3 ^(c,e)	39.8±2.8 ^(c,e)	14.4±3.9 ^(d)	12.6±4.4 ^(c,e)	15.2±0.8	12±3.4 ^(c)	14.4±3.9	51.2±7.4 ^(a,b,b,c,d,e)	21.2±4.1 ^(a,b,b,c,e)	30±3.3 ^(c,d,e)	1.1	

Values are presented as mean±SD. ANOVA *post hoc* test. C+ve, positive control; C-ve, negative control. ^{a)} P<0.05 compared to control groups. ^{b)} P<0.05 compared to Metformin treated group. ^{c)} P<0.05 compared to diabetic group. ^{d)} P<0.05 compared to diabetic plus insulin treated group. ^{e)} P<0.05 compared to diabetic plus metformin treated group.

cesses. The basement membrane is a relatively homogeneous layer. A thin peripheral layer of endothelial cytoplasm is located between the basement membrane and the capillary lumen that showing characteristic interruptions (Fig. 5). The epithelial lining of proximal convoluted tubules revealed intact brush border with closely packed, long and regularly shaped microvilli. Cytoplasm contains plenty of mitochondria, apical pinocytic vesicles, and lysosomes. The nucleus is basal, round to oval and contains euchromatic chromatin. The basement membrane is homogeneous and intact (Fig. 6). Distal convoluted tubule epithelial cells showed apical rounded and euchromatic nuclei and short blunt microvilli. Cytoplasm revealed plenty of mitochondria that chiefly located in the basal region of the cell (Fig. 7).

Metformin treated group

Histological examination of the foetal kidneys H&E, PAS, and Toluidine blue stained sections showed the same findings as control group without any changes or abnormalities.

Ultrastructure of foetal kidneys showed the same findings as control group.

Diabetic group

H&E stained sections revealed glomerular changes including shrunken and empty glomeruli, increased corpuscular space, marked vacuolar degeneration, pyknotic nuclei, and haemorrhage. Proximal and distal convoluted tubules showed degeneration of epithelial cell lining, pyknotic nuclei, vacuolation, and shedding of the brush border proximal convoluted tubules (Fig. 2). Examination of PAS stained sections revealed faint reactions in most of the Bowman’s capsules and renal tubules (Fig. 3). Toluidine blue stained sections revealed loss in the normal architecture of the cortex, early immature stages of glomerular development and glomerular changes including shrunken and empty glomeruli, marked vacuolar degeneration and haemorrhage. Proximal and distal convoluted tubules also showed marked vacuolar degeneration of epithelial cell lining (Fig. 4).

The electron microscopic examination of the renal glomerulus revealed areas of thinned glomerular filtration barrier and absence of fenestrations of the endothelial layer and other areas showed thickened lamina densa part of glomerular filtration barrier. Podocytes shows areas of complete loss of foot processes, areas of effacement and widening of foot processes and faint and chromatin clumping in the nuclei. Moreover, there is a reduction of mesangial tissue around the filtration

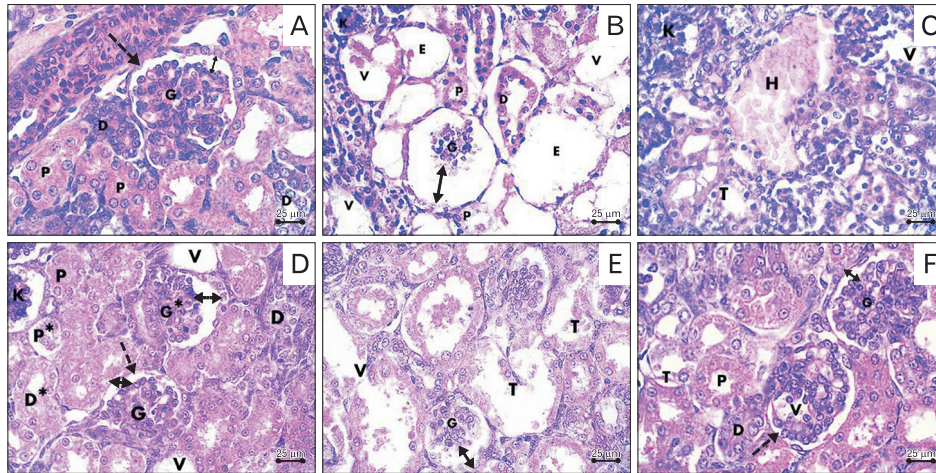


Fig. 2. Photomicrographs sections in the fetal kidney. (A) Control group showing the renal corpuscle with the parietal layer of Bowman's capsule (dashed arrow), mature glomerulus (G) and preserved corpuscular space (double head arrow), proximal (P) and distal (D) convoluted tubules. (B, C) Diabetic group showing shrunken glomerulus (G), increased renal corpuscular space (double head arrow), vacuolations (V), empty renal corpuscles (E), degenerated dilated tubules (T), shedding of brush border of proximal tubules (P), degenerated epithelium of distal tubule (D), hemorrhage (H) and pyknotic nuclei (K). (D) Diabetic plus insulin-treated group showing intact mature glomeruli (G) surrounded by Bowman's capsule (dashed arrow) with preserved corpuscular space (double head arrow), intact proximal (P) and distal tubules (D). Notice the presence of mildly shrunken glomerulus (G*), pyknotic nuclei (K), increased corpuscular space (double head dashed arrow), degenerated proximal (P*) and distal convoluted tubules (D*) and areas of vacuolation (V). (E) Diabetic plus metformin-treated group showing shrunken mature glomerulus (G), increased renal corpuscular space (double head arrow), dilated and destructed renal tubules (T), and vacuolation (V). (F) Diabetic plus insulin and metformin-treated group showing intact glomeruli (G), Bowman's capsule (dashed arrow), and preserved corpuscular space (double head arrow), intact proximal (P) and distal (D) convoluted tubules. Notice the presence of areas of vacuolation in the glomerulus (V) and tubules (T) (H&E staining, $\times 400$).

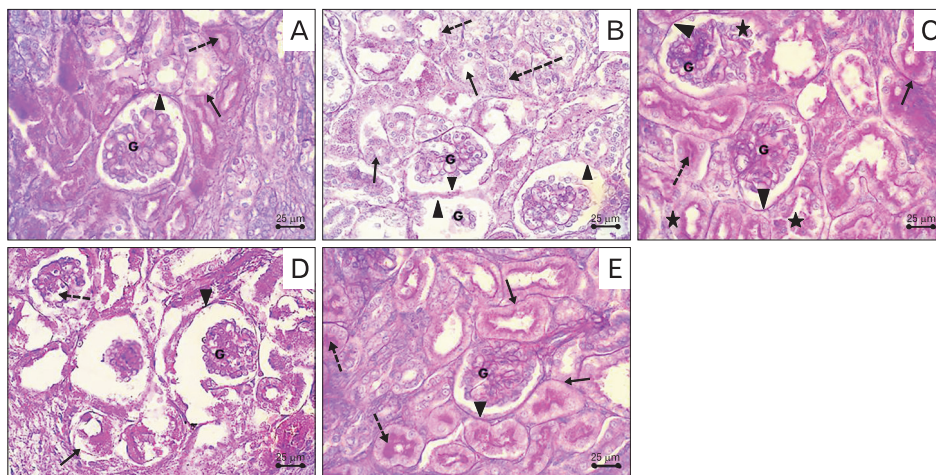


Fig. 3. Periodic acid-Schiff stained sections in the fetal kidney. (A) Control group showing positive stain in the glomeruli (G), Bowman's capsule (arrowhead), basement membrane of renal tubules (arrow) and the brush border of proximal tubules (dashed arrow). (B) Diabetic group showing faint reaction in glomeruli (G), Bowman's capsules (arrowheads), basement membrane (dashed arrows) and brush border of the proximal convoluted tubules (arrows). (C) Diabetic plus insulin treated group showing positive reaction in the glomeruli (G), Bowman's capsule (arrowheads), basement membrane of renal tubules (arrow) and the brush border of proximal tubules (dashed arrow). Notice the presence of areas of negative reaction (stars). (D) Diabetic plus metformin treated group showing areas of faint reaction in the tubular basement membrane (arrow) and glomerulus (dashed arrow) with the presence of positive reaction in other glomerulus (G) and Bowman's capsule (arrowhead). (E) Diabetic plus insulin and metformin treated group showing positive reaction in the glomerulus (G), Bowman's capsule (arrowhead), basement membrane of renal tubules (arrows) and the brush border of proximal tubules (dashed arrows) (periodic acid-Schiff, $\times 400$).

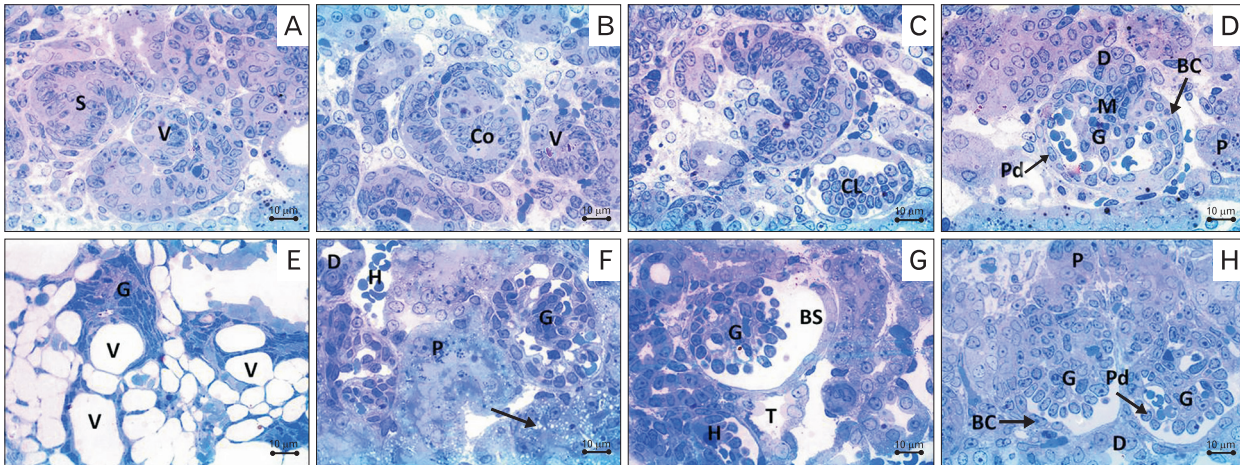


Fig. 4. Photomicrographs of Toluidine blue stained sections in the fetal kidney. (A–C) Control group showing vesicle (V), S-shaped (S), comma-shaped (Co), and capillary loop (CL) stages of glomerular development. (D) Control group showing mature glomerulus (G) with the parietal layer of Bowman’s capsule (BC), podocyte (Pd), mesangial cells (M), proximal convoluted tubules (P) and distal (D) convoluted tubules. (E) Diabetic group showing, loss in the normal architecture of the cortex, immature glomerulus (vesicular stage) (G) and marked vacuolations (V) within the glomerulus and tubules. (F) Diabetic plus insulin-treated group showing intact mature glomerulus (G), proximal (P) and distal (D) convoluted tubules. Notice small area of hemorrhage (H) and vacuolation (arrow). (G) Diabetic plus metformin-treated group showing shrunken glomerulus (G), wide Bowman’s space (BS), and areas of hemorrhage (H). Notice degenerated tubules (T). (H) Diabetic plus insulin and metformin-treated group showing intact mature renal glomerulus (G), Bowman’s capsule (BC), podocyte (Pd), proximal (P) and distal (D) convoluted tubules (toluidine blue, $\times 1,000$).

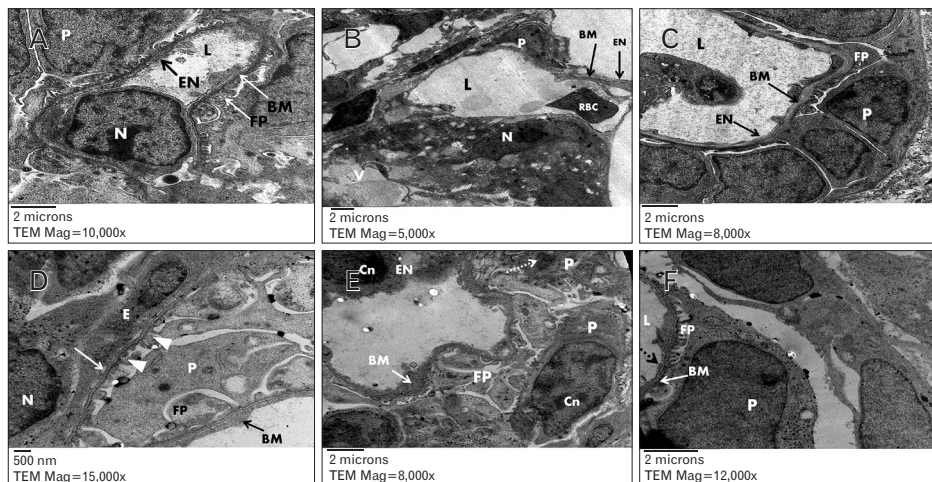


Fig. 5. Electron photomicrographs in fetal rat glomerulus. (A) Control group showing glomerular capillary lumen (L) lined with endothelial cell with euchromatic nucleus (N) and forming a thin fenestrated layer of cytoplasm (EN) lining the basement membrane (BM) internally. The capillary surrounded with intact podocyte (P) with foot processes (FP). Uranyl acetate and lead citrate ($\times 10,000$). (B) Diabetic group showing glomerular capillary lumen (L) with thinned glomerular filtration barrier (BM) and red blood cell (RBC), absence of fenestrations of endothelial layer (EN), vacuolations (V), podocytes with loss of foot processes (P) and chromatin clumping (N). Uranyl acetate and lead citrate, $\times 5,000$. (C) Diabetic group showing glomerular capillary lumen (L) with a thickened glomerular basement membrane (BM) and area of absence of EN and surrounded by podocyte (P) with short foot process effacement and widening (FP). Uranyl acetate and lead citrate, $\times 8,000$. (D) Diabetic plus insulin-treated group showing capillary endothelial cell (E) with euchromatic nucleus (N), podocyte (P) with intact foot processes (arrowheads) and homogeneous glomerular basement membrane with normal thickness (white arrow). Other areas of thickened glomerular basement membrane (BM) and marked widening and effacement of foot processes (FP). Uranyl acetate and lead citrate, $\times 15,000$. (E) Diabetic plus metformin-treated group showing area of thick glomerular basement membrane (BM) and chromatin condensation (Cn) in nuclei of capillary endothelial cell (EN) and podocytes (P). Notice the presence of ill-defined nuclear envelop (dashed arrow) and foot process with effacement and widening (FP). Uranyl acetate and lead citrate, $\times 8,000$. (F) diabetic plus insulin and metformin-treated group showing glomerular capillary lumen (L), intact glomerular basement membrane (BM), podocytes (P) with narrow and short foot processes (FP), thin layer of cytoplasmic endothelium with characteristic interruptions (dashed arrow). Uranyl acetate and lead citrate, $\times 12,000$.

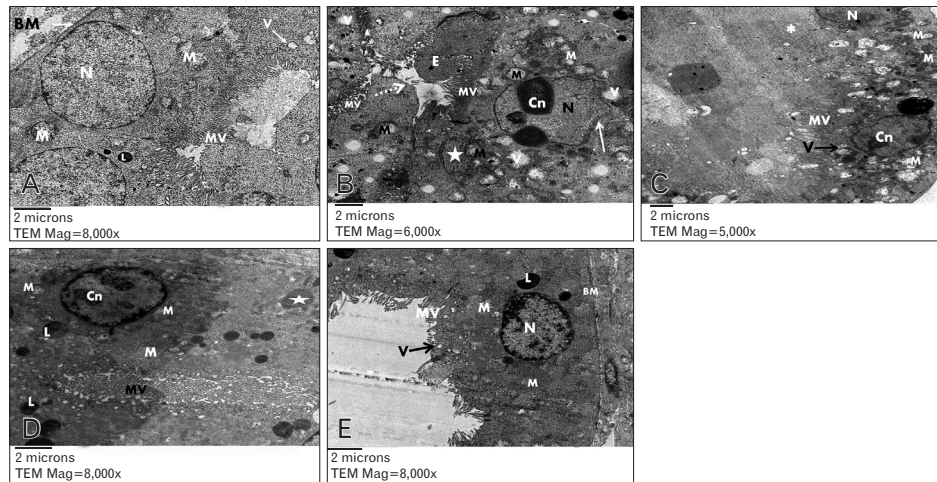


Fig. 6. Electron photomicrographs in the proximal convoluted tubule epithelial cells of fetal rat kidney. (A) Control group showing basal eu chromatic nucleus (N), apical brush border with closely packed microvilli (MV), pinocytotic vesicles (V), lysosome (L), plenty of mitochondria (M) and basement membrane (BM). Uranyl acetate and lead citrate, $\times 8,000$. (B) Diabetic group showing irregular shaped nucleus (N), ill-defined and irregular nuclear envelope (white arrow), chromatin condensation (Cn), apical sticky and profoundly thin microvilli (MV) with areas of total loss of brush border (dashed arrow), swollen mitochondria with disruption of cristae (M) and apoptotic body (star). Notice presence of pinocytotic vesicles (V), and the lumen filled with exudate (E). Uranyl acetate and lead citrate, $\times 6,000$. (C) Diabetic plus insulin treated group showing closely packed apical long microvilli (MV), eu chromatic nucleus (N) and plenty of mitochondria (M). Notice the presence of areas with microvilli loss (*), vesicles (V), and nucleus with chromatin condensation (Cn). Uranyl acetate and lead citrate, $\times 5,000$. (D) Diabetic plus metformin treated group showing plenty of lysosomes (L), edematous mitochondria (M), nucleus with chromatin condensation (Cn), apoptotic body (star) and apical profoundly thin and sloughed microvilli (MV). Uranyl acetate and lead citrate, $\times 8,000$. (E) Diabetic plus insulin and metformin-treated group showing closely packed apical microvilli (MV), pinocytotic vesicles (V), lysosomes (L), eu chromatic nucleus (N), plenty of mitochondria (M) and intact basement membrane (BM). Uranyl acetate and lead citrate, $\times 8,000$.

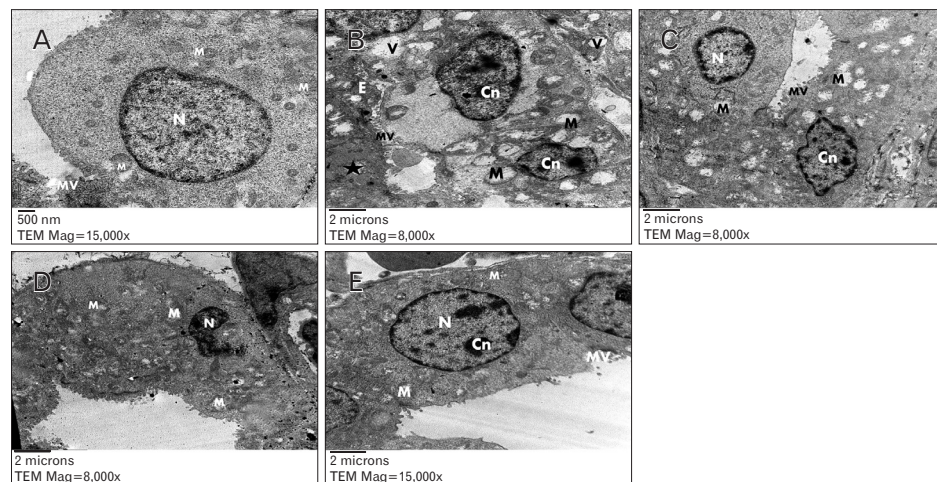


Fig. 7. Electron photomicrographs in the distal convoluted tubule epithelial cells of fetal rat kidney. (A) Control group showing with blunt microvilli (MV), rounded eu chromatic nucleus (N) and plenty of mitochondria (M). Uranyl acetate and lead citrate, $\times 15,000$. (B) Diabetic group showing lumen obliteration with exudate (E), few microvilli (MV), swollen and disrupted mitochondria (M), pinocytotic vesicles (V), apoptotic body (star) and nuclei with chromatin condensation (Cn). Uranyl acetate and lead citrate, $\times 8,000$. (C) Diabetic plus insulin-treated group showing short apical microvilli (MV), eu chromatic nucleus (N) while other nucleus showed chromatin condensation (Cn), swollen and disrupted mitochondria (M). Uranyl acetate and lead citrate, $\times 8,000$. (D) Diabetic plus metformin-treated group showing ill-defined cell boundaries, swollen mitochondria (M) and destructed and ruptured nucleus (N). Uranyl acetate and lead citrate, $\times 8,000$. (E) Diabetic plus insulin and metformin-treated group showing small microvilli (MV), eu chromatic rounded nucleus (N) with chromatin condensation (Cn) and intact mitochondria (M). Uranyl acetate and lead citrate, $\times 8,000$.

barrier and vacuolations (Fig. 5). The proximal convoluted tubule epithelial cell lining revealed irregular nuclei with ill-defined nuclear envelope and chromatin condensation. Moreover, the brush border showed apical sticky and profoundly thin microvilli with areas of total loss and most of mitochondria are swollen and showed disrupted cristae. Furthermore, tubal lumina are obliterated with exudate. There are apoptotic bodies, lysosomes and pinocytotic vesicles (Fig. 6). The distal convoluted tubule epithelial cells show chromatin condensation, swollen disrupted cristae of mitochondria, apoptotic bodies, lysosomes, and pinocytotic vesicles and obliterated lumen with exudate (Fig. 7).

Diabetic plus insulin-treated group

Light microscopic examination of H&E-stained sections revealed that most of sections showed intact and mature renal corpuscles, proximal and distal convoluted tubules. Few areas showed vacuolation, pyknotic nuclei, shrunken glomerulus, increased corpuscular space, and degenerated proximal and distal convoluted tubules (Fig. 2). Most of PAS stained sections revealed positive reaction in the glomeruli, Bowman's capsule, basement membrane of tubules and brush border of the proximal convoluted tubules and few areas showed faint reaction (Fig. 3). Most of toluidine blue stained sections revealed intact and mature renal corpuscles, proximal and distal convoluted tubules with the presence of few areas of vacuolations, hemorrhage and degenerated proximal and distal convoluted tubules (Fig. 4).

Ultrastructure of most of the glomeruli showed intact podocytes and capillary endothelial cells. Glomerular basement membrane showed homogeneity and normal thickness. Few glomerular areas revealed thickening in endothelial part of the glomerular basement membrane and widening and effacement of foot processes of podocytes (Fig. 5). Convoluted tubule epithelial cells showed intact organelles and apical long microvilli with the presence of few areas of microvilli loss, swollen and disrupted mitochondria with disruption of cristae and nuclei with chromatin condensation (Figs. 6, 7).

Diabetic plus metformin-treated group

H&E-stained sections revealed increased early immature forms of renal corpuscles, the presence of shrunken and empty glomeruli, congested glomerular capillaries, increased corpuscular space, haemorrhage, vacuolation and degenerated renal tubules. Few renal corpuscles showed mature glomeruli and preserved renal space (Fig. 2). Most of PAS

stained sections showed positive reaction with the presence of some scattered areas of faint PAS reaction (Fig. 3). Toluidine blue stained sections revealed increased immature forms of glomerular development, shrunken and empty glomeruli, congested glomerular capillaries, increased corpuscular space, haemorrhage, vacuolations and degenerated renal tubules and brush border loss (Fig. 4).

Ultrastructure of glomeruli revealed the presence of areas of thick glomerular basement membrane, nuclear changes of podocytes in the form of chromatin condensation and ill-defined nuclear envelope. Podocytes also showed wide and short foot process. The capillary endothelial cells revealed nuclear chromatin condensation (Fig. 5). Moreover, convoluted tubule epithelial cells showed profoundly thin and sloughed microvilli, oedematous mitochondria, plenty of lysosomes, chromatin condensation in nuclei and the presence of apoptotic body (Figs. 6, 7).

Diabetic plus insulin and metformin treated group

Most of H&E-stained sections of the fetal kidneys showed different forms of immature renal corpuscles, more maturation of glomeruli and intact proximal and distal tubules close to the features of control group, with the presence of few areas of degenerated tubular epithelial cells and glomeruli (Fig. 2). Examination of PAS stained sections showed positive PAS reaction (Fig. 3). Toluidine blue stained sections revealed intact glomeruli, proximal and distal tubules close to the features of control group, with the presence of scanty areas of degenerated tubular epithelial cells (Fig. 4).

Ultrastructure of glomeruli in this group showed intact and homogenous glomerular basement membrane, intact podocytes, capillary endothelium, proximal and distal convoluted tubule epithelial cells close to the features of control group. Few cells showed chromatin condensation in their nuclei. Many pinocytotic vesicles were also evident in the cytoplasm (Figs. 5–7).

Discussion

GDM outcomes present a serious and increasing global challenge. Babies born to hyperglycaemic women are at greater risk of foetal abnormalities. Diabetic embryopathy affects developing organs, including the urinary system, producing congenital renal malformations, which usually occur in early organogenesis, such as renal agenesis, hydronephrosis and ureteric abnormalities [22].

The diabetic group in the current study showed hyperglycemia from the time of the induction until GD20. Moreover, a decline in the RBS levels was also observed in diabetic plus insulin, diabetic plus metformin and diabetic plus insulin and metformin-treated groups with the best and closest value to the control in the diabetic plus insulin and metformin treated group followed by diabetic plus insulin treated group. These results were in agreement with the finding of a previous study reported that metformin decrease the hyperglycaemia through reducing glucose output from the liver and augmenting glucose uptake in the peripheral tissues [23].

Although mono therapy with an oral hypoglycaemic agent is often initially effective, glycaemic control deteriorates in most of the patients with high secondary failure rates which require the addition of a second agent [24]. Furthermore, a combination of metformin and insulin was reported to reduce HbA1c in patients sub-optimally controlled by diet and exercise and improve glycaemic control [25].

The present study also revealed significant increase in the number of post-implantation loss in the diabetic and diabetic plus metformin-treated groups. Diabetic plus insulin and diabetic plus insulin and metformin-treated groups showed significant decrease in the number of resorptions compared to other diabetic groups, with more improvement in the combination group. This result was in agreement with other studies; as they observed that uncontrolled GDM confer specific fetal risks include spontaneous abortion, increased perinatal mortality and preterm birth [26]. On the other hand, Singh et al. [27] observed absence of perinatal mortality among pregnant women with GDM treated with metformin in prospective non-randomized interventional study.

The current study revealed a significant increase in fetal and placental weight in diabetic group. Diabetic plus insulin, diabetic plus metformin and diabetic plus insulin and metformin-treated groups showed a significant decrease in the fetal and placental weight compared to the diabetic group, with the best improvement in combination group. These results are in accordance with previous studies that reported that GDM affect placental and fetal growth as Taricco et al. [28], they found an increase in the placental weight in GDM. Ornoy [29] mentioned that intrauterine growth restriction occurs primarily in the fetuses of severely diabetic mothers. The increased risk of accelerated growth and macrosomia is mainly due to the increased IR of the mother, high maternal glycaemia, plasma amino acid concentrations, and uptake of amino acids at the placental level; so the higher amount of glucose passes

through the placenta into the foetal circulation and stored as fat causing macrosomia [30]. Moreover, insulin treatment was reported to be associated with increased risk of hypoglycemia and weight gain in GDM. While metformin exerts its clinical effect by both reducing hepatic glucose output, increasing glucose utilization and increasing insulin sensitivity, resulting in a decrease in glucose level without an associated high risk of either hypoglycemia or weight gain [31]. Accordingly, these results may explain the best foetal and placental weights in diabetic plus insulin and metformin-treated group in the current study.

Regarding the foetal kidney size in the present study, the kidney length and width were significantly increased in the diabetic group. Diabetic plus insulin and diabetic plus metformin-treated groups showed a reduction in the kidney size compared to diabetic group and the best results achieved in the combination group. This finding is in accordance with previous studies that reported the existence of renal hypertrophy and hyperfunction in DM clinically and experimentally. Maternal hyperglycaemia induce foetal hyperinsulinemia that lead to increased cellular glucose utilization, increased fat deposition and protein production, leading to overgrowth and increased cell size [32]. Other mechanisms involve some fibroblast growth factors and insulin-like growth factors, as their concentrations have been demonstrated to be high in GDM that are commonly associated with organomegally [33]. Moreover, it was concluded that the best glycaemic effect of combination of insulin and metformin protects the fetal kidney from the deleterious effects of GDM [14].

In the current study, the glomerular morphometric parameters in diabetic group revealed an increase in renal corpuscular diameters whereas; the glomerular diameters were significantly decreased indicating the occurrence of glomerular shrinkage with dilatation of the corpuscular space. Moreover, the tubular morphometric parameters in diabetic group showed increased tubular diameters due to dilatation of both proximal and distal convoluted tubules. Furthermore, all renal morphometric parameters showed mild improvement in the diabetic plus metformin treated group, moderated in the diabetic plus insulin treated group and marked improvement in the combination group.

Glomerular atrophy was reported to be a result of loss or inadequate circulation of nephrons, as the renal veins and arteries start to shrink leading to glomerular shrinkage [34]. Moreover, Dodd [35] mentioned that the initial tubular epithelial cell hypertrophy is considered “compensatory” and

“adaptive” hypertrophy, in which the hypertrophic cells are arrested in the G1-phase of the cell cycle and increase protein and RNA content, but do not replicate their DNA.

Diabetic group in the current study also revealed retardation of glomerular development in the form of increased immature stages of glomeruli and consequently the immature/mature glomerular ratio. This result is in accordance with [36], they reported that DM can cause changes in the number of proliferating renal cells and also increased production of collagen and other extracellular matrix components. Alterations in extracellular matrix (ECM) composition will impair the nephrogenesis in pups of hyperglycemic mothers, as the ECM formation is a key event in renal cell differentiation and the severity of fetal changes depend on cell differentiation stage at the time that the mother develops GDM [37].

Furthermore, the mature renal corpuscles in the diabetic group in present study revealed shrunken and empty glomeruli with increased corpuscular space, vacuolar degeneration and hemorrhage. The convoluted tubules showed degeneration of epithelial cells, vacuolar degeneration and shedding of the brush border. These findings are in disagreement with Nobrega et al. [38], as they observed hypertrophy in the glomeruli, and narrowing in the Bowman’s space in diabetic group. On the other hand, the results of Gonzalez Suarez et al. [39] and Zini et al. [40] were in accordance with those of the present study.

Previous studies explained the mechanism of occurrence of these histopathological alterations by the effects of STZ administration. The metabolism of the STZ molecule leads to the induction of unscheduled DNA synthesis and damage in kidney cells and radical oxygen species (ROS) [41].

Moreover, Floege et al. [42] reported that glomerular atrophy may result from the toxic effect of the free radicals on the mesangial cells and affect its function causing glomerular contraction, decreased the mesangial matrix secretion and further glomerular atrophy. Other study explained the glomerular changes by neutrophil activation as the first line responders in inflammation and ROS, proteases, cytokines, and chemokines [43].

Some authors observed that glycogen granules accumulation in about half of the distal tubules that associated with sustained hyperglycemia. The glycogen accumulation in the tubules was known to induce apoptosis of the tubular cells which led to a compensatory renal hypertrophy characterized by an increase in tubule diameter [40].

The ultrastructure of foetal kidneys in the diabetic group

in this study revealed glomerular changes include vacuolation, thickened lamina densa, loss of foot processes and chromatin condensations in podocytes and reduction of mesangial tissue. They also showed changes in tubular epithelial cells, nuclear chromatin condensation, ill-defined nuclear envelope mitochondrial edema and destruction, apoptotic bodies and loss of brush border. These results are in agreement with Weil et al. [44]. Moreover, Kumar et al. [45] reported that hyperglycemia directly mediates apoptotic cell death which explains the chromatin condensation and the presence of apoptotic bodies in the epithelial cells of renal tubules in the present study. Furthermore, some authors reported that podocytes cultured under high-glucose conditions died via apoptosis as the release of mitochondrial and plasma membrane ROS played an important role in its damage. When podocytes are lost the remaining podocytes adapt to extend coverage over the newly denuded glomerular basement membrane (GBM) leading to podocyte hypertrophy [46].

Diabetic plus insulin treated group in the current study revealed increased glomerular maturity, intact mature renal corpuscles, proximal and distal convoluted tubules. Areas of vacuolation, shrunken glomeruli and degenerated tubules were still present. Moreover, the ultrastructure of most of the glomeruli and epithelial cells of renal tubules showed normal cytoplasmic organelles, nuclei and GBM, whereas, few places of thickened GBM, widening of podocyte foot processes, loss of microvilli, swollen mitochondria and chromatin condensation were observed.

Moreover, insulin was reported to play an important role in glomeruli-genesis through increasing the bioavailability of insulin-growth factor (IGF), overexpression of IGF-binding proteins, conditional transgene expression of IGF and increasing IGF2-receptor oligonucleotides [47, 48]. These findings could explain the maturation and improvement of renal corpuscles and tubules in fetal kidneys of the diabetes plus insulin treated group in our study.

On the other hand, fetal kidneys of diabetic plus metformin treated group in the present study revealed delayed glomerular maturation in the form of increased early immature figures of glomeruli and decreased mature ones with increased immature/mature glomerular ratio. They also showed hemorrhage, vacuolations, shrunken and empty glomeruli, dilated corpuscular spaces, degenerated renal tubules. Few areas showed preservation of mature corpuscles and faint PAS reaction. The ultrastructure of fetal kidneys showed areas of glomerular changes such as thick GBM, chromatin condensa-

tion, ill-defined nuclear envelope and short foot process in podocytes. Tubular epithelial cells changes were found in the form of thin and sloughed brush border, oedematous mitochondria, plenty of lysosomes, chromatin condensation, ill-defined cell boundaries and the presence of apoptotic body. These results indicate that metformin did not ameliorate the effects of GDM on the fetal kidneys. Crowther et al. [49] were in disagreement with these results as they reported the absence of increased incidence of perinatal complications or congenital anomalies in patients treated with metformin compared with those received insulin.

Moreover, Moore et al. [50] concluded that women with GDM treated with metformin had improved neonatal outcomes compared with those treated with insulin. Morales et al. [51] found that metformin had a renal protective action and ameliorated gentamicin-induced renal tubular injury. Furthermore, some authors reported that metformin reduced diabetes-induced podocyte loss. Additionally, previous studies have recognized that metformin possesses antioxidant effects, to reduce apoptosis, in endothelial cells as well as inhibition of vascular endothelial cell dysfunction [52]. Finally, the beneficial action of this drug is known to be achieved through activation of adenosine monophosphate-activated protein kinase, that plays an important role in protecting cellular function and inhibition of mitochondrial respiratory chain [53]. Metformin was also reported to decrease the risk of neonatal hypoglycemia [54].

Munshi and Khandaker [55] compared the efficacy of metformin versus insulin in GDM patients and mentioned that insulin produce good glycemic control in 84% of patient whereas, metformin achieved euglycemic state in 72% of patients. This may explain the better results of diabetic plus insulin treated group when compared with diabetic plus metformin treated group in the present study.

Fetal kidneys in diabetic plus insulin and metformin-treated group in the current study showed improvement of maturation and structure of glomeruli and tubules, homogenous GBM and intact podocytes. Some authors concluded that the combination of insulin and metformin resulted in superior glycemic control and decreased insulin requirements. Moreover, previous studies reported that high insulin levels induce DNA damage and the combination of metformin with insulin protects kidneys from oxidative stress and genomic damage [14].

Conclusion

The present study showed that STZ induced GDM adversely affects the pregnancy outcome and fetal kidney development and possess marked hazardous impact on fetal kidneys. Prenatal treatment with insulin improves the glycemic state, ameliorates and decreases the side effects of GDM on fetal kidneys. Treatment with metformin produces mild fetal kidneys protection. The combination of insulin and metformin produces the best glycemic control and reduced to greater extent the toxic effect of STZ induced GDM on the fetal kidneys. Further studies will be needed for assessing the mechanisms by which the combined treatment with insulin and metformin induce restoration and preservation of fetal kidney structure and development.

References

1. World Health Organization. Definition, diagnosis and classification of diabetes mellitus and its complications: report of a WHO consultation. Part 1. Diagnosis and classification of diabetes mellitus. Geneva: World Health Organization; 1999.
2. Scherzer P, Katalan S, Got G, Pizov G, Londono I, Gal-Moscovici A, Popovtzer MM, Ziv E, Bendayan M. Psammomys obesus, a particularly important animal model for the study of the human diabetic nephropathy. *Anat Cell Biol* 2011;44:176-85.
3. King AJ. The use of animal models in diabetes research. *Br J Pharmacol* 2012;166:877-94.
4. Winocour PH. Diabetes and chronic kidney disease: an increasingly common multi-morbid disease in need of a paradigm shift in care. *Diabet Med* 2018;35:300-5.
5. Buchanan TA, Xiang AH, Page KA. Gestational diabetes mellitus: risks and management during and after pregnancy. *Nat Rev Endocrinol* 2012;8:639-49.
6. Guariguata L, Linnenkamp U, Makaroff LE, Ogurtsova K, Colagiuri S. Global estimates of hyperglycaemia in pregnancy: determinants and trends. In: Rajendram R, Preedy VR, Patel VB, editors. *Nutrition and Diet in Maternal Diabetes: An Evidence-Based Approach*. Cham: Springer International Publishing; 2018. p.3-15.
7. Fetita LS, Sobngwi E, Serradas P, Calvo F, Gautier JF. Consequences of fetal exposure to maternal diabetes in offspring. *J Clin Endocrinol Metab* 2006;91:3718-24.
8. Graham DL, Schaefer TL, Vorhees CV. Neurobehavioral testing for developmental toxicity. In: Hood RD, editor. *Developmental and Reproductive Toxicology: A Practical Approach*. Boca Raton, FL: CRC Press; 2016. p.346-87.
9. Alfadhli EM. Gestational diabetes mellitus. *Saudi Med J* 2015;36:399-406.
10. Pilmore HL. Review: metformin: potential benefits and use in chronic kidney disease. *Nephrology (Carlton)* 2010;15:412-8.
11. Legro RS. Metformin during pregnancy in polycystic ovary syn-

- drome: another vitamin bites the dust. *J Clin Endocrinol Metab* 2010;95:5199-202.
12. Balani J, Hyer SL, Rodin DA, Shehata H. Pregnancy outcomes in women with gestational diabetes treated with metformin or insulin: a case-control study. *Diabet Med* 2009;26:798-802.
 13. Rowan JA, Rush EC, Obolonkin V, Battin M, Wouldes T, Hague WM. Metformin in gestational diabetes: the offspring follow-up (MiG TOFU): body composition at 2 years of age. *Diabetes Care* 2011;34:2279-84.
 14. Othman EM, Oli RG, Arias-Loza PA, Kreissl MC, Stopper H. Metformin protects kidney cells from insulin-mediated genotoxicity in vitro and in male Zucker diabetic fatty rats. *Endocrinology* 2016;157:548-59.
 15. Varayoud J, Ramos JG, Bosquiazzo VL, Lower M, Muñoz-de-Toro M, Luque EH. Neonatal exposure to bisphenol A alters rat uterine implantation-associated gene expression and reduces the number of implantation sites. *Endocrinology* 2011;152:1101-11.
 16. Amorim EM, Damasceno DC, Perobelli JE, Spadotto R, Fernandez CD, Volpato GT, Kempinas WD. Short- and long-term reproductive effects of prenatal and lactational growth restriction caused by maternal diabetes in male rats. *Reprod Biol Endocrinol* 2011;9:154.
 17. Ikeda T, Iwata K, Murakami H. Inhibitory effect of metformin on intestinal glucose absorption in the perfused rat intestine. *Biochem Pharmacol* 2000;59:887-90.
 18. Pan Y, Li YJ, Zhao HY, Zheng JM, Xu H, Wei G, Hao JS, Cui FD. Bioadhesive polysaccharide in protein delivery system: chitosan nanoparticles improve the intestinal absorption of insulin in vivo. *Int J Pharm* 2002;249:139-47.
 19. Ellis EN, Steffes MW, Goetz FC, Sutherland DE, Mauer SM. Relationship of renal size to nephropathy in type 1 (insulin-dependent) diabetes. *Diabetologia* 1985;28:12-5.
 20. Suvarna SK, Layton C, Bancroft JD. Bancroft's theory and practice of histological techniques. Philadelphia, PA: Elsevier Health Sciences; 2012.
 21. Furuse A, Bernstein J, Welling LW, Welling DJ. Renal tubular differentiation in mouse and mouse metanephric culture. II. Na-K-ATPase activity. *Pediatr Nephrol* 1989;3:273-9.
 22. Guariguata L, Linnenkamp U, Makaroff LE, Ogurtsova K, Colagiuri S. Global estimates of hyperglycaemia in pregnancy: determinants and trends. In: Rajendram R, Preedy VR, Patel VB, editors. *Nutrition and Diet in Maternal Diabetes: Nutrition and Health*. Cham: Humana Press; 2018. p.3-15.
 23. Shaw RJ, Lamia KA, Vasquez D, Koo SH, Bardeesy N, Depinho RA, Montminy M, Cantley LC. The kinase LKB1 mediates glucose homeostasis in liver and therapeutic effects of metformin. *Science* 2005;310:1642-6.
 24. Turner RC, Cull CA, Frighi V, Holman RR. Glycemic control with diet, sulfonylurea, metformin, or insulin in patients with type 2 diabetes mellitus: progressive requirement for multiple therapies (UKPDS 49). UK Prospective Diabetes Study (UKPDS) Group. *JAMA* 1999;281:2005-12.
 25. Lund SS, Tarnow L, Frandsen M, Nielsen BB, Hansen BV, Pedersen O, Parving HH, Vaag AA. Combining insulin with metformin or an insulin secretagogue in non-obese patients with type 2 diabetes: 12 month, randomised, double blind trial. *BMJ* 2009;339:b4324.
 26. Martinez CA. The ultrasound evaluation of the diabetic pregnancy. In: Moore L, editor. *Diabetes in Pregnancy*. Cham: Springer; 2018. p.163-81.
 27. Singh N, Madhu M, Vanamail P, Malik N, Kumar S. Efficacy of metformin in improving glycaemic control & perinatal outcome in gestational diabetes mellitus: a non-randomized study. *Indian J Med Res* 2017;145:623-8.
 28. Taricco E, Radaelli T, Nobile de Santis MS, Cetin I. Foetal and placental weights in relation to maternal characteristics in gestational diabetes. *Placenta* 2003;24:343-7.
 29. Ornoy A. Embryonic oxidative stress as a mechanism of teratogenesis with special emphasis on diabetic embryopathy. *Reprod Toxicol* 2007;24:31-41.
 30. Liu F, Zhao C, Liu L, Ding H, Huo R, Shi Z. Peptidome profiling of umbilical cord plasma associated with gestational diabetes-induced fetal macrosomia. *J Proteomics* 2016;139:38-44.
 31. Ainuddin JA, Karim N, Zaheer S, Ali SS, Hasan AA. Metformin treatment in type 2 diabetes in pregnancy: an active controlled, parallel-group, randomized, open label study in patients with type 2 diabetes in pregnancy. *J Diabetes Res* 2015;2015:325851.
 32. Neves HM, Sgarbosa F, Calderon IM, Vianna LS, Santini AC, Sieiro Netto L, Dias A. Does hyperglycemia in pregnancy change fetal kidney growth? A longitudinal prospective study. *Rev Bras Ginecol Obstet* 2013;35:442-6.
 33. Page NM, Kemp CF, Butlin DJ, Lowry PJ. Placental peptides as markers of gestational disease. *Reproduction* 2002;123:487-95.
 34. Venkatachalam MA, Griffin KA, Lan R, Geng H, Saikumar P, Bidani AK. Acute kidney injury: a springboard for progression in chronic kidney disease. *Am J Physiol Renal Physiol* 2010;298:F1078-94.
 35. Dodd SM. Tubulointerstitial and cystic disease of the kidney. Berlin: Springer Science & Business Media; 2012.
 36. Kolset SO, Reinholt FP, Jenssen T. Diabetic nephropathy and extracellular matrix. *J Histochem Cytochem* 2012;60:976-86.
 37. Battin M, Wouldes TA, Rowan J. Neurodevelopmental outcome in offspring born following gestational diabetes. In: Rajendram R, Preedy V, Patel V, editors. *Nutrition and Diet in Maternal Diabetes: Nutrition and Health*. Cham: Humana Press; 2018. p.341-54.
 38. Nobrega MA, Fleming S, Roman RJ, Shiozawa M, Schlick N, Lazar J, Jacob HJ. Initial characterization of a rat model of diabetic nephropathy. *Diabetes* 2004;53:735-42.
 39. Gonzalez Suarez ML, Thomas DB, Barisoni L, Fornoni A. Diabetic nephropathy: is it time yet for routine kidney biopsy? *World J Diabetes* 2013;4:245-55.
 40. Zini E, Benali S, Coppola L, Guscetti F, Ackermann M, Lutz TA, Reusch CE, Aresu L. Renal morphology in cats with diabetes mellitus. *Vet Pathol* 2014;51:1143-50.
 41. Friesen NT, Buchau AS, Schott-Ohly P, Lgssiar A, Gleichmann H. Generation of hydrogen peroxide and failure of antioxidative responses in pancreatic islets of male C57BL/6 mice are associated with diabetes induced by multiple low doses of streptozotocin.

- Diabetologia 2004;47:676-85.
42. Floege J, Eng E, Young BA, Johnson RJ. Factors involved in the regulation of mesangial cell proliferation *in vitro* and *in vivo*. *Kidney Int Suppl* 1993;39:S47-54.
 43. Kitching AR, Hutton HL. The players: cells involved in glomerular disease. *Clin J Am Soc Nephrol* 2016;11:1664-74.
 44. Weil EJ, Lemley KV, Yee B, Lovato T, Richardson M, Myers BD, Nelson RG. Podocyte detachment in type 2 diabetic nephropathy. *Am J Nephrol* 2011;33 Suppl 1:21-4.
 45. Kumar D, Zimpelmann J, Robertson S, Burns KD. Tubular and interstitial cell apoptosis in the streptozotocin-diabetic rat kidney. *Nephron Exp Nephrol* 2004;96:e77-88.
 46. Inoki K, Mori H, Wang J, Suzuki T, Hong S, Yoshida S, Blattner SM, Ikenoue T, Ruegg MA, Hall MN, Kwiatkowski DJ, Rastaldi MP, Huber TB, Kretzler M, Holzman LB, Wiggins RC, Guan KL. mTORC1 activation in podocytes is a critical step in the development of diabetic nephropathy in mice. *J Clin Invest* 2011;121:2181-96.
 47. Gross ML, Amann K, Ritz E. Nephron number and renal risk in hypertension and diabetes. *J Am Soc Nephrol* 2005;16 Suppl 1: S27-9.
 48. Sison KT. Role of VEGF and VEGF receptors in the glomerulus [thesis]. Toronto: University of Toronto; 2009.
 49. Crowther CA, Hiller JE, Moss JR, McPhee AJ, Jeffries WS, Robinson JS; Australian Carbohydrate Intolerance Study in Pregnant Women (ACHOIS) Trial Group. Effect of treatment of gestational diabetes mellitus on pregnancy outcomes. *N Engl J Med* 2005;352:2477-86.
 50. Moore LE, Briery CM, Clokey D, Martin RW, Williford NJ, Bofill JA, Morrison JC. Metformin and insulin in the management of gestational diabetes mellitus: preliminary results of a comparison. *J Reprod Med* 2007;52:1011-5.
 51. Morales AI, Detaille D, Prieto M, Puente A, Briones E, Arevalo M, Leverve X, Lopez-Novoa JM, El-Mir MY. Metformin prevents experimental gentamicin-induced nephropathy by a mitochondria-dependent pathway. *Kidney Int* 2010;77:861-9.
 52. Tavafi M. Diabetic nephropathy and antioxidants. *J Nephro-pathol* 2013;2:20-7.
 53. Gobe GC, Morais C, Vesey DA, Johnson DW. Use of high-dose erythropoietin for repair after injury: A comparison of outcomes in heart and kidney. *J Nephro-pathol* 2013;2:154-65.
 54. Balsells M, García-Patterson A, Solà I, Roqué M, Gich I, Corcoy R. Glibenclamide, metformin, and insulin for the treatment of gestational diabetes: a systematic review and meta-analysis. *BMJ* 2015;350:h102.
 55. Munshi S, Khandaker S. Evaluation of metformin versus insulin in the management of gestational diabetes mellitus: a prospective comparative study. *Int J Reprod Contracept Obstet Gynecol* 2017;3:357-61.